THE ELECTRICAL AND OPTICAL PROPERTIES OF THIN FILM DIAMOND IMPLANTED WITH SILICON

K. J. Roe and J. Kolodzey
Department of Electrical and Computer Engineering, University of Delaware, Newark, DE 19716

C. P. Swann
Bartol Research Institute, University of Delaware, Newark, DE 19716

M.W. Tsao, J. F. Rabolt, J. Chen
Department of Materials Science and Engineering, University of Delaware, Newark, DE 19716

G. R. Brandes
Advanced Technology Materials Inc., Danbury, CT 06810

Abstract

The superb mechanical and electrical properties of diamond make it an attractive material for use in extreme conditions. Diamond devices have been fabricated, but the combination of diamond with other materials to form alloys is not yet well understood. We have investigated the electrical and optical properties of diamond implanted with Si, which is in principle isoelectronic in diamond. The diamond layers were 23 μm thick p-type layers grown on (100) Si substrates. Silicon was implanted at room temperature, at energy of 300keV with doses of up to 8.0×10^{16} cm^{-3}. A two-stage post-implant anneal process was then performed at 500°C for 30 minutes, then 800°C for 30 minutes. Rutherford Backscattering Spectrometry (RBS) measurements indicated Si concentrations up to 2 atomic percent, in agreement with simulations of implant profiles. X-ray measurements indicated that about 60-70% of the Si was incorporated substitutionally, corresponding to up to 1.5 atomic percent from linear interpolation of lattice constants. Raman Spectroscopy measurements confirmed that the diamond structure was reconstructed with the post-implant anneal treatment. NEXAFS measurements confirmed the reconstruction of the sp^3 diamond bonds from sp^2 graphite after annealing. Electrical measurements indicated an increase in diode current density with increased Si dose and a decrease in contact resistance with contact anneals. These novel diamond alloys may be useful for electronic and optical devices. We report on the preparation and properties of these alloys.

Keywords: diamond, implantation, alloys, XRD, RBS, Raman, heterostructure

Corresponding Author:
Kristofer Roe
Department of Electrical and Computer Engineering
140 Evans Hall, University of Delaware
Newark, DE 19716
(302) 831-8959 phone
(302) 831-4316 fax
e-mail: roe@ee.udel.edu

Background

As a wide bandgap (E_g = 5.45 eV) semiconductor material, diamond has promise for use in high-voltage and high-power devices. Diamond layers could function well as a wide-bandgap emitter, if a suitable second material existed for the formation of heterostructure devices. There are many applications where the superior power handling, friction coefficient, mechanical strength, and exceptional hardness properties of diamond would give an advantage over Si or GaAs technologies. Here we report on a C:Si alloy, formed by the implantation of Si into diamond. Si implantation in diamond has been used at low doses for formation of stoichiometric SiC for the improvement of metal contacts [1]. In this case we have larger concentrations of Si that change the lattice structure and other properties, indicating a $C_{1-x}Si_x$ alloy. This new alloy holds promise as a new material for use with diamond to make new and novel heterostructure devices.

The C:Si alloys were formed by the implantation of Si into polycrystalline diamond films grown by chemical vapor deposition. The diamond film was grown on Si(100) in a hot filament assisted chemical vapor deposition system. The gases for diamond growth: hydrogen (99.99%), methane (10% in UHP H_2) and diborane (2000ppm in UHP H_2) were purified with inline purifiers. The 4" diameter Si(100) substrate was seeded with diamond by polishing thoroughly with a 2μm diamond slurry. Following polishing, the silicon wafer was ultrasonically cleaned, dipped in 1:1 H_2O:HF and dried with a stream of dry N_2 before insertion into the diamond growth reactor. The silicon substrate was rotated to ensure uniform diamond film thickness. The diamond film was ~23μm thick following 229 hours of growth. To remove residual graphite and to ensure hydrogen termination, the hydrogen flow was continued with the filament at growth temperature for 30 min after the carbon and boron gas flows were stopped. After the growth was complete, no extra precautions were taken to avoid exposure to air or ambient humidity.

Si was implanted into the diamond layer at energy of 300keV and a dose range of 1 x 10^{15} cm^{-2} to 8 x 10^{16} cm^{-2}. Graphitization of the samples after implant was observed from Raman measurements. The samples were then annealed with a two-stage treatment after Prins [2]. The first step was 500°C for 30 minutes in N_2 ambient. A greater effect on the diamond structure was observed from the partial reconstruction of the Raman spectra then expected from Prins. Therefore the second step temperature was lowered from the listed value of 1000°C to 800°C for 30 minutes. Raman Spectroscopy and Near Edge X-ray Absorption Fine Structure (NEXAFS) measurements confirmed that the diamond sp^3 structure was reconstructed after annealing. Rutherford Backscattering Spectroscopy (RBS) measurements confirmed up to 2 percent of Si in the implanted samples. X-ray diffraction (XRD) measurements showed an increase in lattice constant, implying that some of the Si was substitutional.

Analysis

Prior to implantation, baseline scans of XRD, RBS, and Raman were performed for subsequent comparison. An unimplanted diamond sample was also processed along with the Si-implanted samples as a reference. SRIM ion implantation simulations were performed to estimate the Si concentration and depth profile. Samples were implanted with Si as listed in Table 1.

X-Ray Diffraction (XRD)

XRD measurements were performed using a Philips X'Pert MRD materials research diffractometer with a CuKα radiation source. The $CuK\alpha_1$ radiation is selected by a four-bounce Ge (220) Bartels monochromator, and a triple-axis output monochromator for high resolution. The system is also equipped with a fully rotational rocking curve stage, which allows measurement of off-axis reflections. Initial XRD measurements showed the films to be highly-ordered polycrystalline, with <111> being the primary (>75% intensity) orientation (See Figure 1). Diamond reflections from (111), (220), and (311) were observed with all samples. Also observed were the (004) and forbidden (002) reflections of the Si substrate, which are observed because of the large penetration depth of the x-rays. The presence of the forbidden (002) Si reflection may indicate SiC formation or mixing at the diamond/Si interface or perhaps the substrate doping. In each case, the layer reflections are referenced to the Si substrate peak present in each scan. The substrate peak is corrected to the nominal value for Si (a = 5.43088Å). Any correction in 2Θ to the measured Si peak is then applied to the 2Θ value of the layer peak. After implantation there was little change in the peak position. After anneal there was a definite shift of the peak towards a lower 2Θ angle indicating a larger lattice constant (see Figure 2). This is consistent with substitutional Si incorporation into the diamond lattice as the lattice constant of Si is much larger than that of diamond (3.5667 Å). Using Vegard's Law, interpolation between the Si and diamond lattice constant yields 1.65% substitutional incorporation of Si. Based on the 2.05% theoretical SRIM concentration, we can estimate 80% substitutional incorporation of Si after anneal. This value is consistent with other measurements as shown later.

Raman Spectroscopy

Raman spectroscopy measurements were performed using a green laser system operating in parallel orientation. Initial Raman spectroscopy measurement of the samples showed the expected diamond peak at 1330 cm^{-1} and a small SiC peak (520 cm^{-1}). We do not see graphite (1520 cm^{-1}) peaks, indicating true diamond growth and graphite removal. After implantation, we see the amorphitization of the sample as expected for our high implant doses (Figure 3, dotted curve). No peaks are evident, save a wide broad signal around the diamond/graphite energy range. After the first anneal step (Figure 3, dashed curve), some evidence of reconstruction of the lattice was evident. Also appearing is a Si peak at 485 cm^{-1}. We believe this to be due to weakly ordered Si bonds which would manifest themselves at slightly lower energy than the ordered 520 cm^{-1} peak. Since this partial reconstruction is significantly more than expected from the literature, we chose to lower the second anneal step temperature from 1000°C to 800°C, to avoid dissipation of the dopant. After the second (800°C) anneal step, we see full reconstruction of the diamond structure, with no graphite present (Figure 3, solid curve). This result indicates that reconstruction is possible for implant doses that exceed the previously reported limits for the critical 'amorphitization threshold' of 1-6 x 10^{15} cm^{-2} listed in the literature [3] for low temperature implantation. This suggests that the Si behaves differently than a dopant and seems to more favorably incorporate into the diamond lattice.

Rutherford Backscattering Spectrometry (RBS)

RBS measurements were done in vacuum with a 2MeV He-ion source. The data was then fit with the RUMP software analysis package. After implantation, RBS measurements verify the implantation of about 2% of Si at a depth of 2500 Å, which is in good agreement with the SRIM

simulations. See Figure 4 for the RBS data after implant. After anneal (Figure 5) RBS suggests that some of the Si has diffused through the grainy polycrystalline diamond structure to the surface. A thin layer of roughly 100Å of SiC was formed at the surface. We also see a buried layer where the Si has incorporated into the reconstructed diamond lattice. RUMP simulation yields a concentration of $C_{0.983}Si_{0.017}$, which is in excellent agreement with the XRD measurements.

Near Edge X-ray Absorption Fine Structure (NEXAFS)

NEXAFS measurements of sample D-14 and D-16 were performed after the second anneal (800°C). See Figure 6 for a plot of the NEXAFS data. The 292.6, 297.8, and 305.2 eV peaks correspond to sp^3 bonds, which comprise the diamond lattice. The 285.6 eV peak corresponds to the graphite sp^2 bond. Note the dominance of the sp^3 bonds, which confirms the reconstruction of the diamond lattice. The graphite bonds may occur in the diffused SiC layer on the surface.

Electrical Characterization

Electrical contacts were formed by e-beam evaporation of Ti/Au directly onto the front and backside of the wafer. The contacts were then annealed in a RTA to 450°C. Devices were formed using a simple circular diode structure, with the backside of the sample as a large area contact. Current-Voltage measurements were performed using a Hewlett Packard 4156 Parameter Analyzer. I-V data was taken before and after contact annealing for comparison. The I-V data after contact anneal is plotted in Figure 7. One should note the clear trend of increasing current with Si concentration. There is also a trend in increasing rectification ratio (forward current / reverse current) with increased Si concentration, indicating heterojunction behavior.

Capacitance voltage measurements were performed using a Hewlett Packard 4284A precision LCR meter in conjunction with the 4156 Parameter Analyzer. C-V measurements were performed on the same circular diode structures. C-V data was taken at a range of frequencies from 100Hz to 1MHz. See Figure 8 for a plot of $1/C^2$ versus voltage for sample D-16 and extrapolated value of Φ_{bi} at 1MHz. The incorporation of Si into the diamond was also found to lower the built-in voltage, but the trend was not as clear as with the I-V measurements.

Conclusions

In this paper we report on a new C:Si alloy formed by ion implantation and annealing. RBS and XRD measurements confirm the substitutional incorporation of Si into the diamond at concentrations of up to 1.7%. Raman and NEXAFS measurements confirm the reconstruction of the diamond lattice even at dose levels above the previously published 'amorphitization limit'. C:Si heterostructure devices have been fabricated and tested. The incorporation of Si into the diamond has been shown to increase currents and decrease the built-in voltages of the heterostructure diodes. These novel diamond alloys may prove useful for electronic and optical devices.

Acknowledgements:

We gratefully acknowledge R. G. Wilson and Dale Jacobson of Bell Labs in Murray Hill, NJ for sample implants and useful discussion.

References:

[1] G. R. Brandes, C. P. Beetz, C. F. Feger, R. W. Wright, and J. L. Davidson, Diamond and Related Materials, v. 8, n 10 (1999) p.1936-1943.

[2] J. F. Prins, Nuclear Instruments and Methods in Physics Research, vol B59/60 (1991) p. 1387-1390.

[3] J. F. Prins, Materials Science and Engineering, B11 (1992) p.219-226.

Figure Captions:

Figure 1. Baseline Θ/2Θ X-ray diffraction scan of unimplanted diamond film. Note the predominance of the <111> orientation. (004) and (002) reflections of the Si substrate are also present.

Figure 2. Comparison of the diamond (111) XRD peak positions after implantation and anneal. Note the shift to lower angle (larger lattice constant) after anneal. Peak positions and corresponding cubic lattice constant are indicated for the peaks.

Figure 3. Raman spectroscopy measurements of sample D-16. The dotted curve shoes the amorphitization of the diamond into graphite after implantation after implant. The dashed curve shows the partial reconstruction of the diamond and graphite phases after the first step of the anneal (500°C). The solid curve illustrates the reconstruction of the diamond lattice structure after the second stage of the anneal (800°C). Peaks at 1550 cm^{-1} and 2330 cm^{-1} are N_2 and O_2, which are present in air in the beam path near the sample stage.

Figure 4. RBS Measurement of sample D-16 after implant. The RUMP fit to the data is shown. The datafit yields an implant layer with depth of 2500A and concentration of $C_{0.98}Si_{0.02}$ as indicated.

Figure 5. RBS Measurement of sample D-16 after second anneal step (800°C). The RUMP fit to the data is shown. Note the incorporation of Si into the diamond lattice at the implant depth, and some diffusion of Si to the surface. RUMP datafit yields a surface SiC layer with thickness of approximately 100Å and a buried layer of concentration $C_{0.983}Si_{0.017}$ at a depth of 2kÅ.

Figure 6. Plot of Near Edge X-ray Absorption Fine Structure (NEXAFS) measurement of sample D-14 and D-16 after second anneal (800°C). The 292.6, 297.8, and 305.2 eV peaks correspond to sp^3 bonds, which are dominant over the 285.6 eV sp^2 bond peak.

Figure 7. Plot of current-voltage characteristics of diamond heterostructure diodes after contact anneal (450°C). Note the increase in current with Si dose.

Figure 8. Plot of capacitance-voltage characteristics of diamond heterostructure diodes after contact anneal (450°C). The extrapolated built-in voltage was found to be 1.28V.

Tables:

Table 1. A summary of implant conditions and SRIM simulated parameters for the sample set. All implants were performed at room temperature and energy of 300 keV.

Sample Number	Si Dose [atoms/cm^2]	SRIM Implant Depth [Å]	SRIM Implant Straggle [Å]	SRIM Si Concentration [%]
D-13	0 (no implant)	0	0	0.0
D-14	1.0×10^{15}	2158	390	0.026
D-15	2.0×10^{16}	2159	391	0.52
D-16	8.0×10^{16}	2174	392	2.05

Table 2. A summary of the current-voltage characteristics of the heterostructure diodes.

SRIM Si Concentration [%]	Forward Current [8V] (mA)	Reverse Current [8V] (mA)	Rectification Ratio
0.026	2.53	2.49	1.02
0.52	15.52	12.73	1.22
2.05	31.56	24.33	1.30

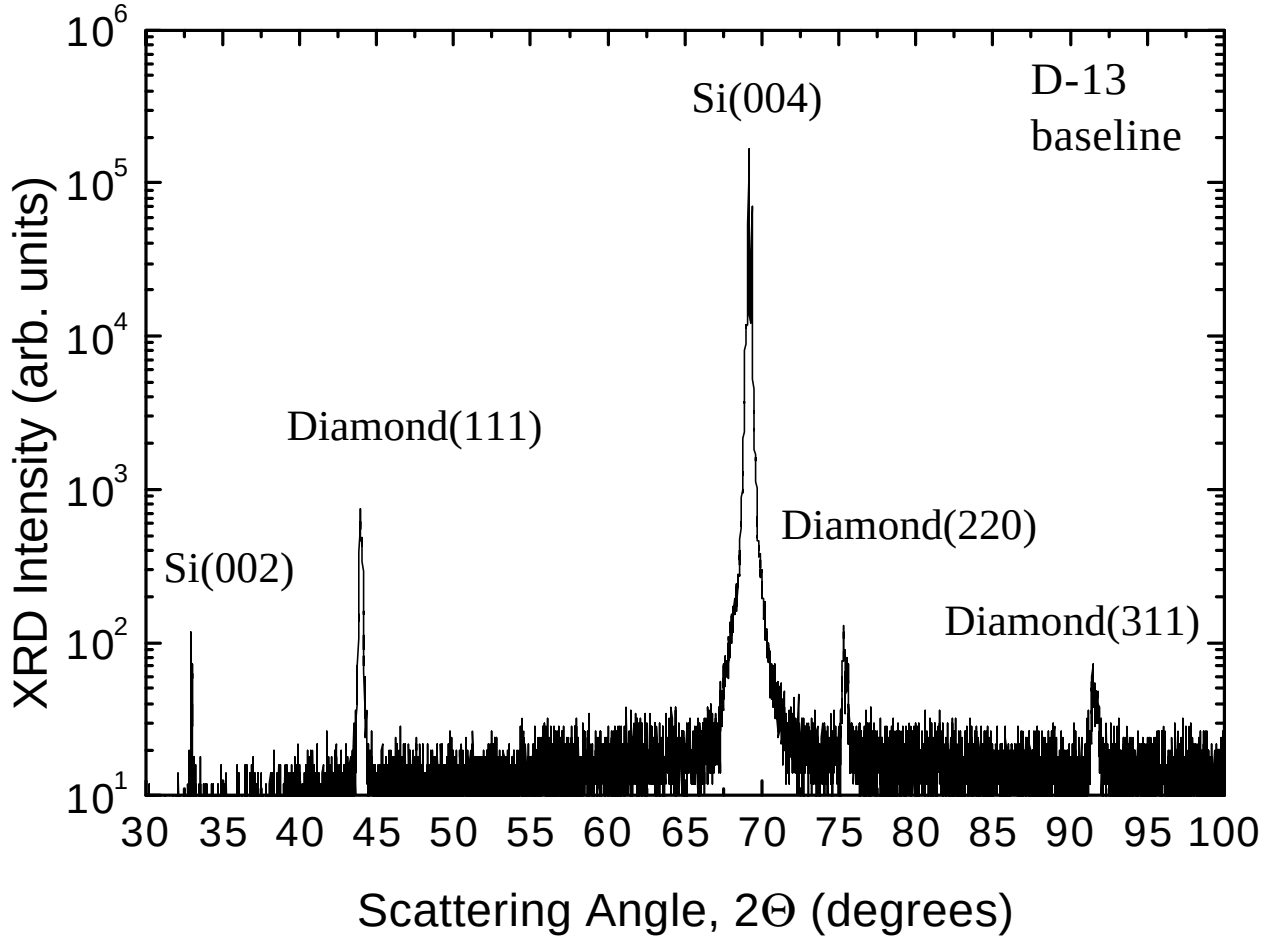
XRD Intensity (arb. units)
Scattering Angle, 2Θ (degrees)
Si(002)
Diamond(111)
Si(004)
Diamond(220)
Diamond(311)
D-13
baseline

Figure 1.

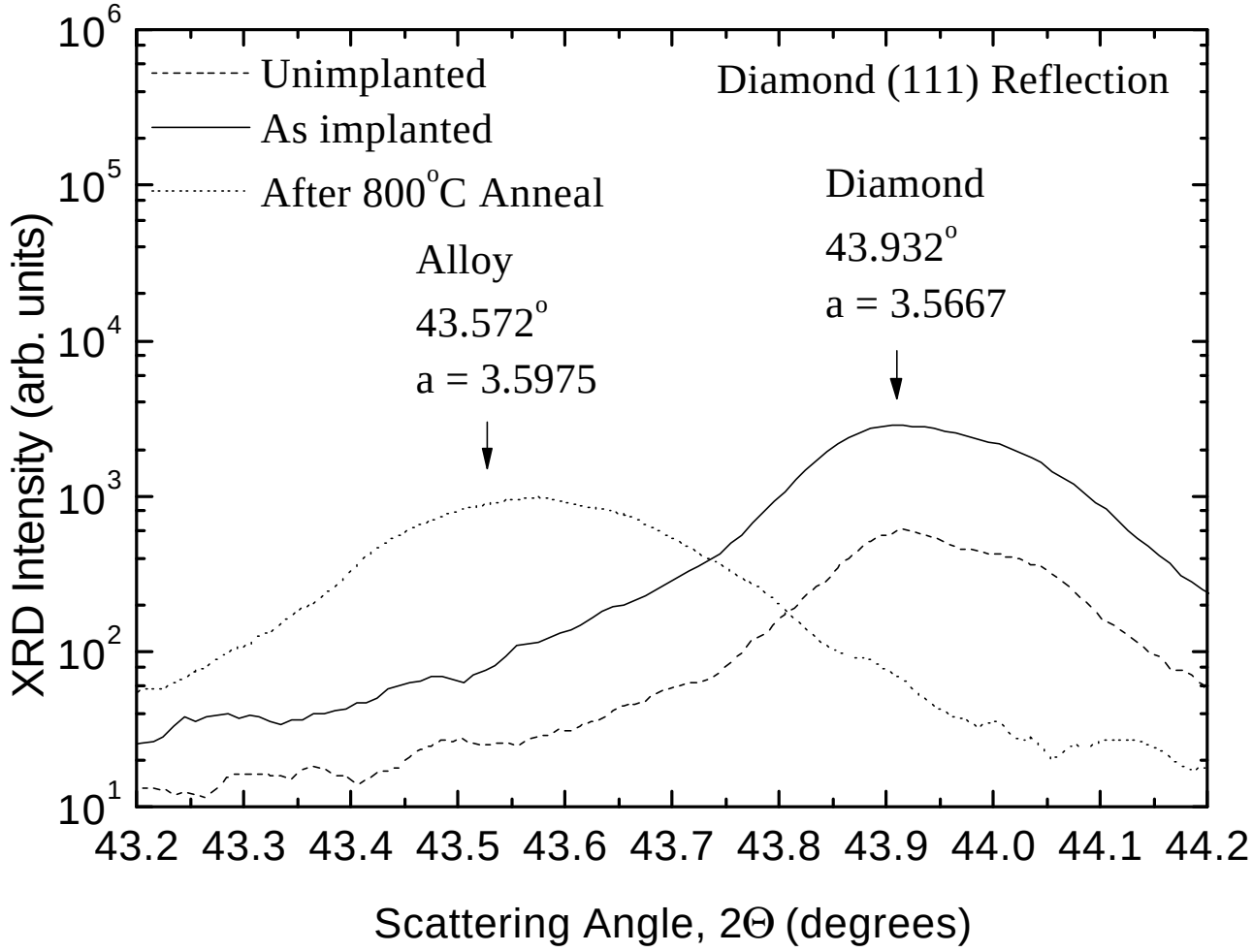
Unimplanted
As implanted
After 800°C Anneal
Diamond (111) Reflection
Diamond
43.932°
a = 3.5667
Alloy
43.572°
a = 3.5975
XRD Intensity (arb. units)
Scattering Angle, 2Θ (degrees)
10^6
10^5
10^4
10^3
10^2
10^1
43.2 43.3 43.4 43.5 43.6 43.7 43.8 43.9 44.0 44.1 44.2

Figure 2.

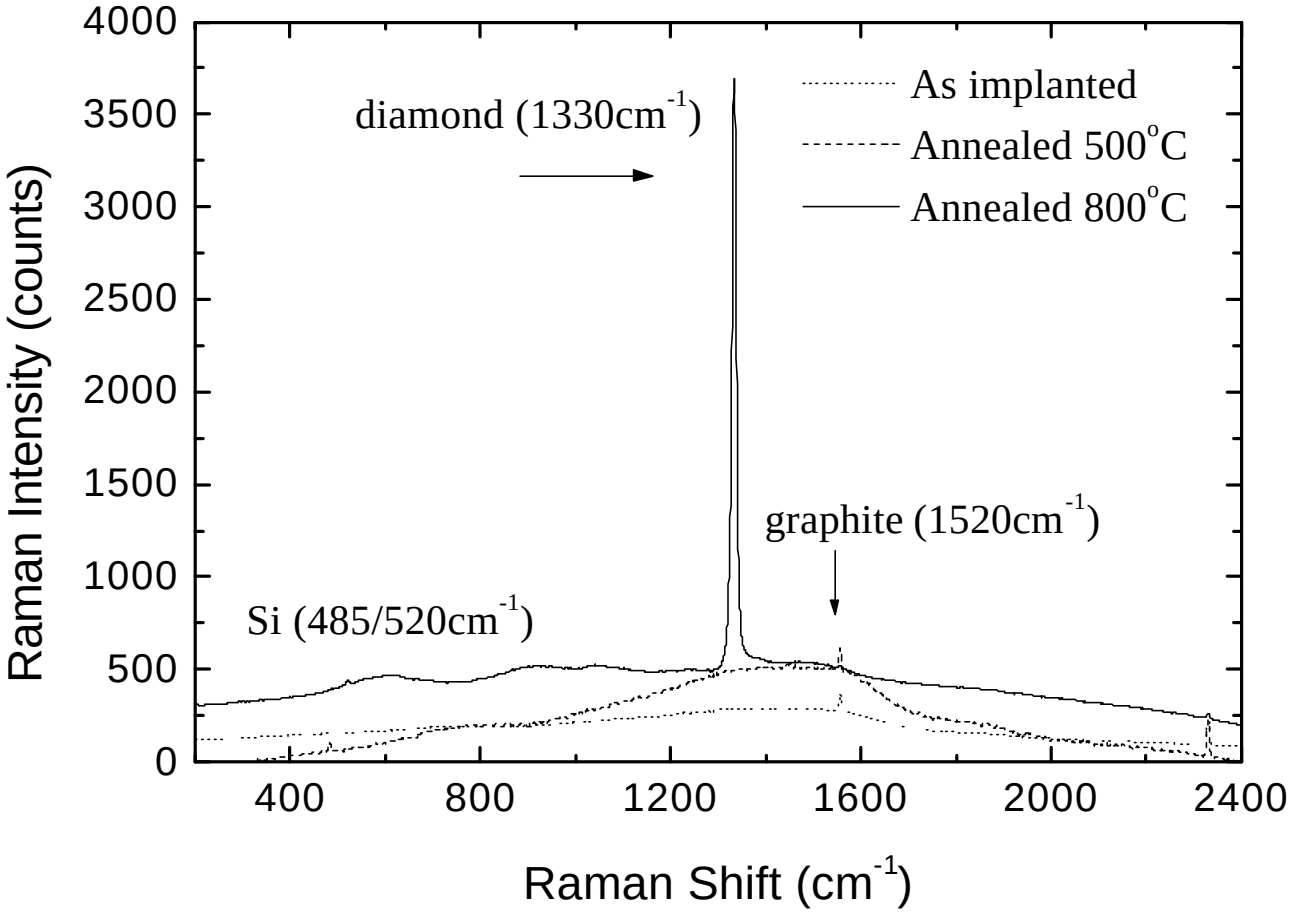
4000
3500
3000
2500
2000
1500
1000
500
0
Raman Intensity (counts)
400
800
1200
1600
2000
2400
Raman Shift (cm-1)
diamond (1330cm-1)
graphite (1520cm-1)
Si (485/520cm-1)
As implanted
Annealed 500°C
Annealed 800°C

Figure 3.

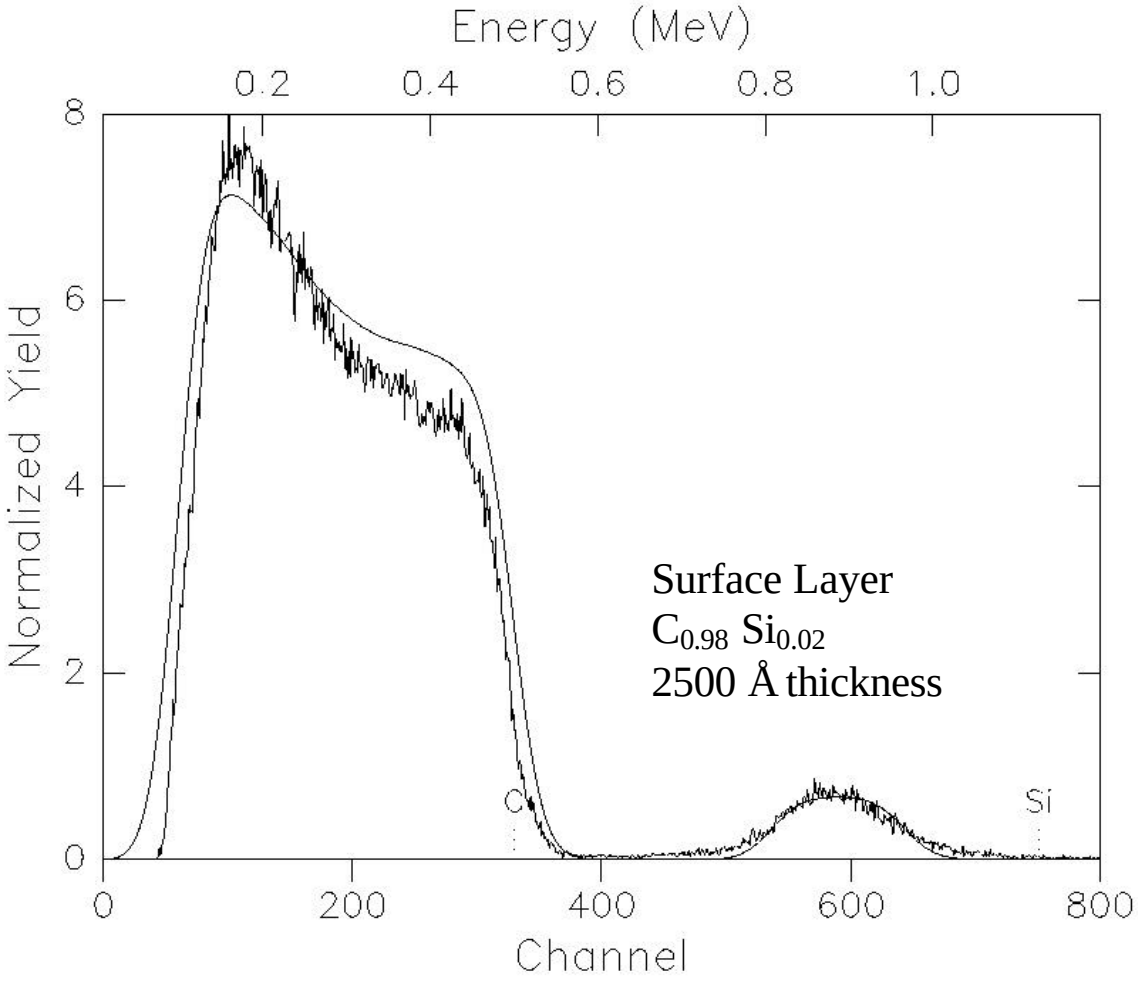
Energy (MeV)
0.2
0.4
0.6
0.8
1.0
Normalized Yield
0
2
4
6
8
0
200
400
600
800
Channel
Surface Layer
$C_{0.98}$ $Si_{0.02}$
2500 Å thickness
C
Si

Figure 4.

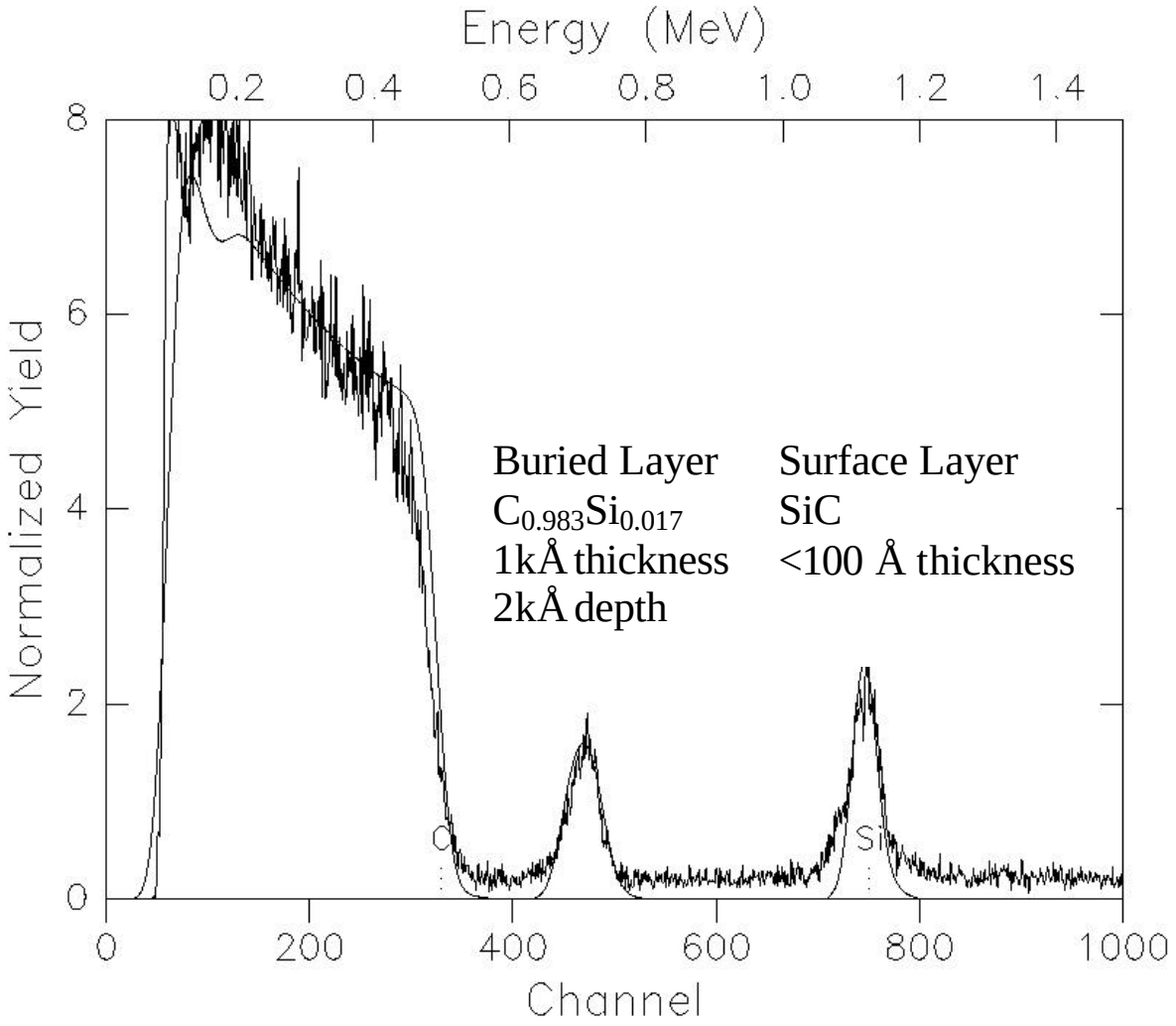
Energy (MeV)
0.2
0.4
0.6
0.8
1.0
1.2
1.4
Normalized Yield
0
2
4
6
8
Buried Layer
$C_{0.983}Si_{0.017}$
1kÅ thickness
2kÅ depth
Surface Layer
SiC
<100 Å thickness
C
Si
0
200
400
600
800
1000
Channel

Figure 5.

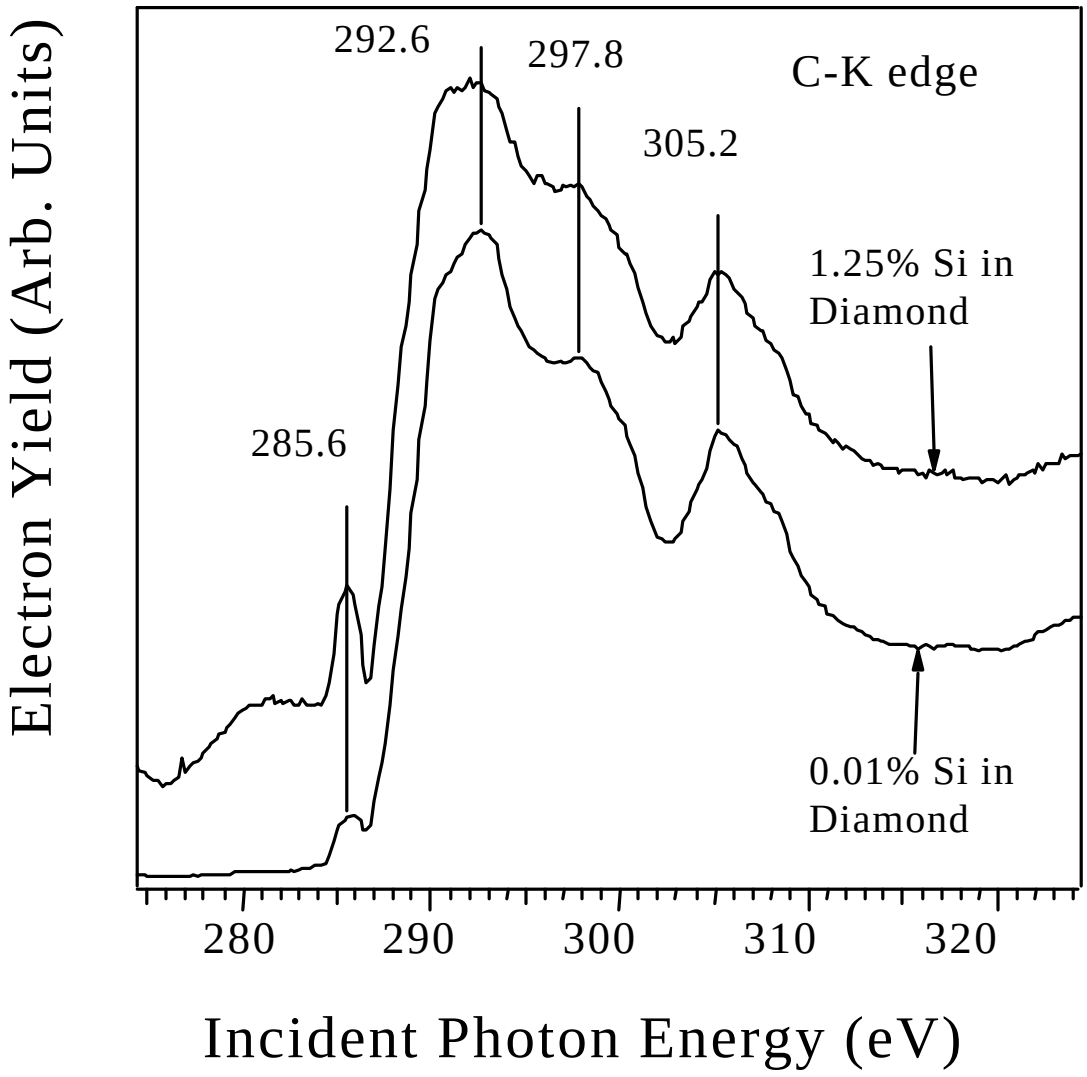
Electron Yield (Arb. Units)
292.6
297.8
305.2
C-K edge
1.25% Si in Diamond
285.6
0.01% Si in Diamond
280
290
300
310
320
Incident Photon Energy (eV)

Figure 6.

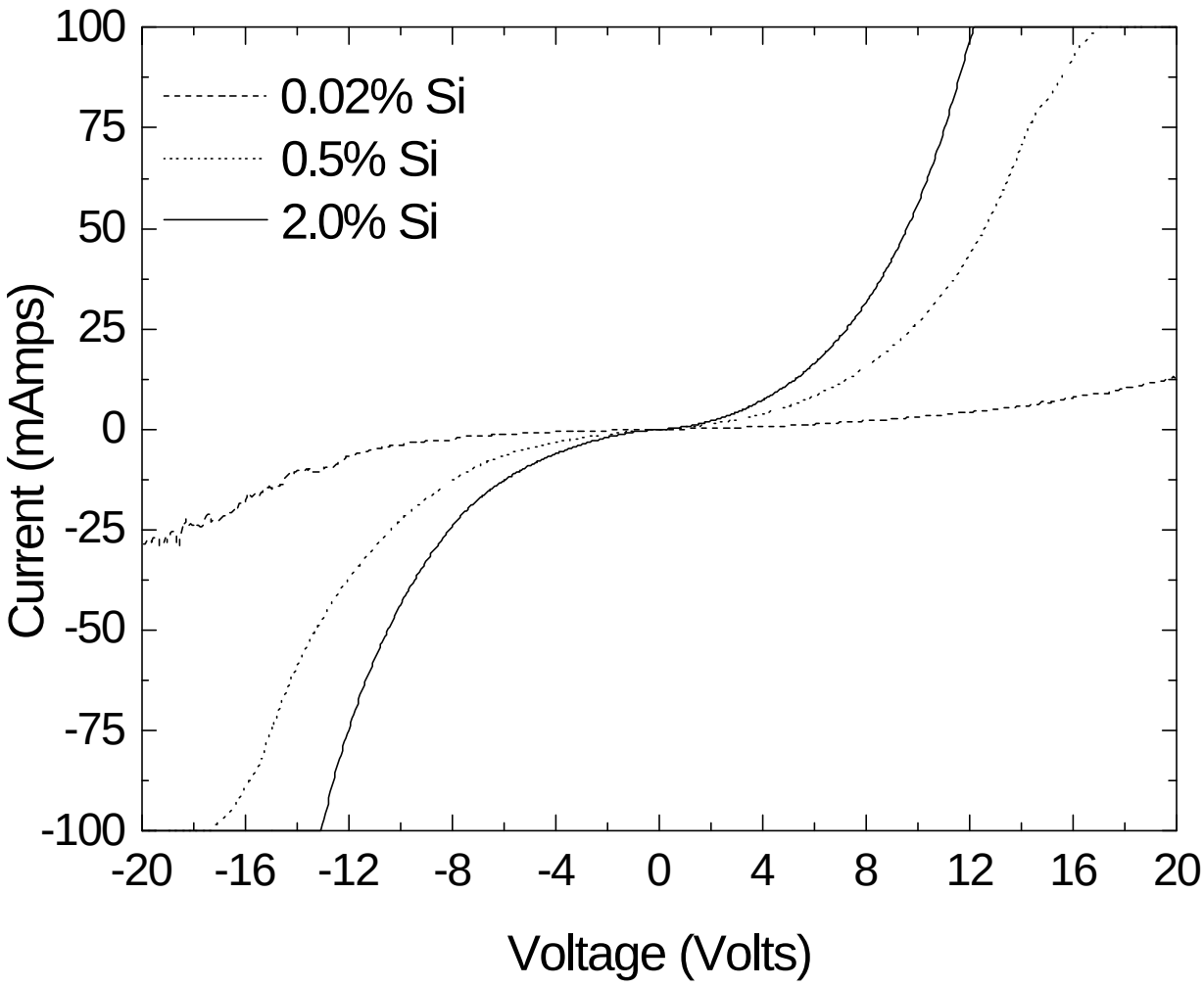
0.02% Si
0.5% Si
2.0% Si
Current (mAmps)
Voltage (Volts)
100
75
50
25
0
-25
-50
-75
-100
-20
-16
-12
-8
-4
0
4
8
12
16
20

Figure 7.

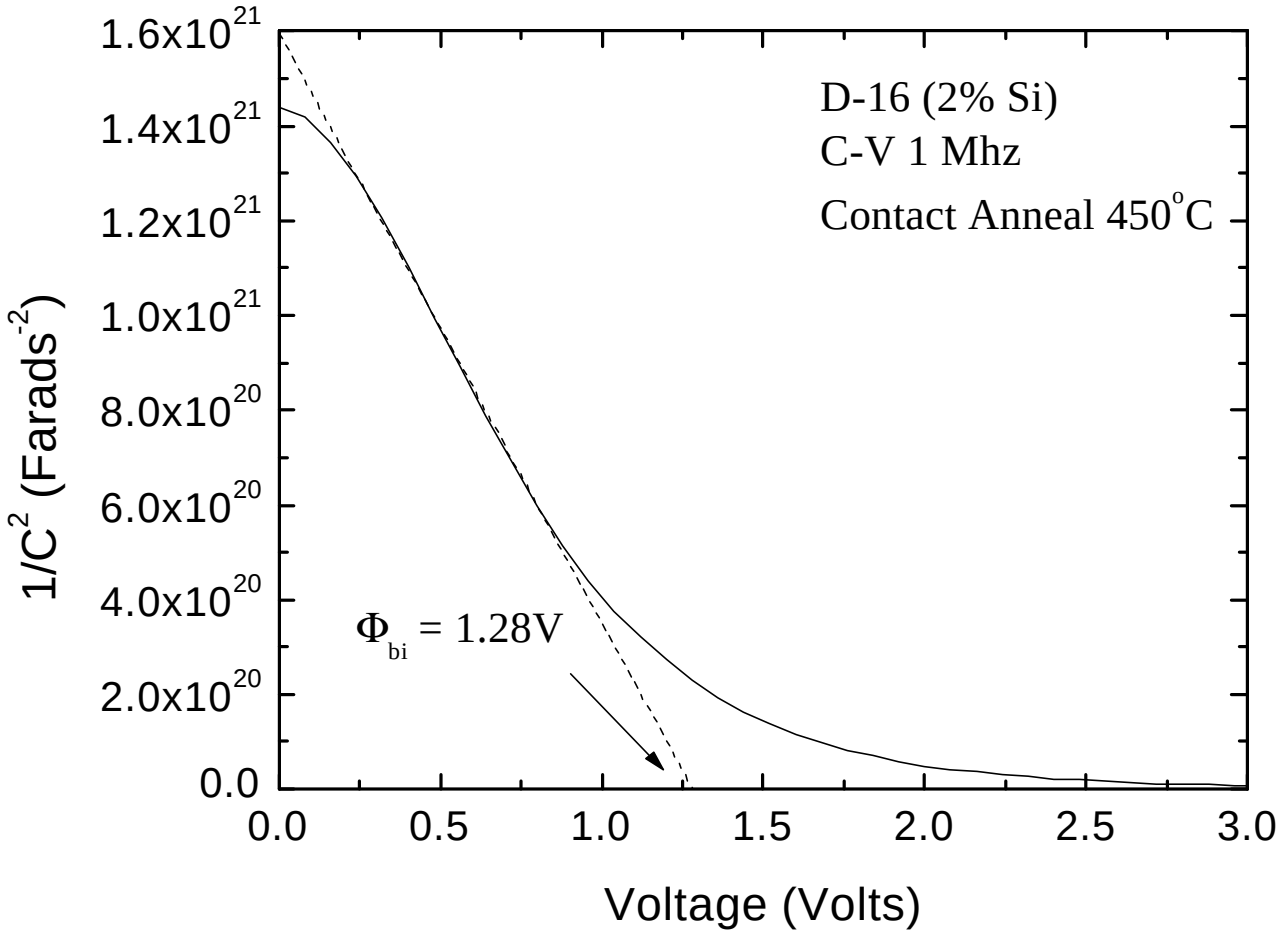
D-16 (2% Si)
C-V 1 Mhz
Contact Anneal 450°C
Φbi = 1.28V
1/C2 (Farads-2)
Voltage (Volts)
1.6x10^21
1.4x10^21
1.2x10^21
1.0x10^21
8.0x10^20
6.0x10^20
4.0x10^20
2.0x10^20
0.0
0.0
0.5
1.0
1.5
2.0
2.5
3.0

Figure 8.